



Communication

Synthesis of polypeptide bearing 1,4-dithiane pendants for ROS-responsive drug release

Tianhui Zhang^{a,b}, Jiuxu Yao^c, Jiamei Tian^c, Mingxiao Deng^c, Xiuli Zhuang^{a,b,e,*}, Chunsheng Xiao^{a,d,e,*}

^a Key Laboratory of Polymer Ecomaterials, Changchun Institute of Applied Chemistry, Chinese Academy of Sciences, Changchun 130022, China

^b University of Science and Technology of China, Hefei 230026, China

^c Department of Chemistry, Northeast Normal University, Changchun 130021, China

^d State Key Laboratory of Molecular Engineering of Polymers, Fudan University, Shanghai 200433, China

^e Jilin Biomedical Polymers Engineering Laboratory, Changchun 130022, China



ARTICLE INFO

Article history:

Received 8 May 2019

Received in revised form 10 June 2019

Accepted 3 July 2019

Available online 3 July 2019

Keywords:

Polypeptides

ROS-responsive

Self-assembly

Thioether

Drug release

ABSTRACT

Stimuli-responsive polypeptides have been intensively investigated for controlled drug release, owing to their favorable biocompatibility and biodegradability. In this work, we designed and synthesized a new kind of polypeptide bearing 1,4-dithiane pendants for reactive oxygen species (ROS)-responsive drug release. The polypeptide-based block copolymer was facilely synthesized by ring-opening polymerization (ROP) of 1,4-dithian-substituted L-glutamate N-carboxyanhydride (DTG-NCA) monomer using an amino-terminated poly(ethylene glycol) methyl ether (mPEG-NH₂) as the macromolecular initiator. The resultant block copolymer, mPEG-*b*-PDTG, could self-assemble into uniform micelles in aqueous medium owing to its amphiphilic structure. Then, the H₂O₂-triggered oxidation behaviors of the mPEG-*b*-PDTG micelles were studied by dynamic light scattering (DLS), FT-IR and turbidimetric assay. It was revealed that the oxidation of thioether into sulfoxide in the side chains would result in disassembly of the micelles. Furthermore, the ROS-responsive drug release behavior of the mPEG-*b*-PDTG micelles was verified by using Nile Red as a model drug. MTT assay also proved that mPEG-*b*-PDTG was non-toxic in B16F10 and L929 cells. Therefore, such a new class of oxidation-responsive polypeptide might provide a promising platform for ROS-responsive drug delivery.

© 2019 Chinese Chemical Society and Institute of Materia Medica, Chinese Academy of Medical Sciences.

Published by Elsevier B.V. All rights reserved.

Poly(α -amino acid)s, also known as synthetic polypeptides, are a kind of polymer with repeated amino acid units in the backbone, which have been intensively used as biocompatible and biodegradable polymers for various biomedical applications, such as drug/gene delivery, antimicrobial and tissue engineering [1–6]. Owing to the same peptide backbone in polypeptides, the physical-chemical properties (such as solubility, chargeability and secondary structure) and even the biological properties of polypeptides are largely dependent on the side chain structure [6–9]. Thus, it is of great importance to prepare polypeptides with side chain functionalities for desirable biomedical applications.

Reactive oxygen species (ROS), including hydrogen peroxide, superoxide, hydroxyl radical, etc., are natural by-products of cell

metabolism, which play important roles in cellular signaling and homeostasis [10,11]. However, increased generation of ROS can cause damages to lipid, proteins and DNA in cells, which is closely associated with various pathologies, such as inflammation, cancer and cardiovascular diseases [12,13]. Based on the elevated ROS level, a number of ROS-responsive polymers have been prepared and used for targeted delivery of drugs to diseased tissues or cells [14–18]. To date, ROS-responsive polypeptides are mainly prepared through ring-opening polymerization (ROP) of alkylated derivatives of cysteine and homocysteine N-carboxyanhydride (NCA) monomers, which have one ROS-responsive thioether group in each side chain. For example, Deming *et al.* prepared glycopolypeptides *via* ROP of glycosylated L-cysteine NCA monomers and the obtained polymers exhibited an oxidation-triggered helix-to-coil transition in aqueous solution [19]. Similarly, OEGylated L-cysteine and L-homocysteine polypeptides were also synthesized, which displayed multimodal conformation-switching and oxidation/thermo-dual responsive properties [20,21]. In addition, Li *et al.* reported the synthesis of oxidation/thermo-dual responsive

* Corresponding authors at: Key Laboratory of Polymer Ecomaterials, Changchun Institute of Applied Chemistry, Chinese Academy of Sciences, Changchun 130022, China

E-mail addresses: zhuangxl@ciac.ac.cn (X. Zhuang), xiaocs@ciac.ac.cn (C. Xiao).

polypeptides with OEG side-chains through thiol-ene and thiol-yne reaction mediated post-polymerization modifications [22,23]. Nevertheless, few efforts have been devoted to the development of ROS-responsive polypeptides for controlled drug release [24,25].

Here, we report the design and synthesis of a new class of ROS-responsive polypeptide *via* ROP of 1,4-dithian-2-yl-methanol (DTM) substituted α -glutamate NCA (DTG-NCA) monomer (Scheme 1). By using an amino-terminated methoxy poly(ethylene glycol) (mPEG-NH₂) as the macromolecular initiator, an amphiphilic block copolymer, mPEG-*b*-PDTG, was synthesized, which could self-assemble into micelles in aqueous media. The resultant mPEG-*b*-PDTG micelles exhibited structural disintegration upon treatment with H₂O₂ and the oxidation mechanism was further studied by ¹H NMR and FT-IR spectrum. Finally, the potential use of mPEG-*b*-PDTG micelles for ROS-responsive drug release was also evaluated by using Nile Red (NR) as a model drug.

The synthetic route for mPEG-*b*-PDTG is depicted in Scheme 1. Firstly, the thioether containing molecule, 1,4-dithian-2-yl-methanol (DTM), was readily synthesized by thiol-yne click reaction between 1,2-ethanedithiol and propargyl alcohol (Scheme S1 in Supporting information). The corresponding structure was confirmed by ¹H NMR and ¹³C NMR spectrum (Figs. S1 and S2 in Supporting information). The DTM was then conjugated with Boc-Glu-OtBu to form Boc-Glu(ODT)-OtBu (Fig. S3 in Supporting information). Subsequently, the Boc-Glu(ODT)-OtBu was deprotected to obtain DTG (Fig. S4 in Supporting information). DTG-NCA was then synthesized by reaction of DTG with triphosgene in THF [26], and the structure of obtained DTG-NCA was confirmed by ¹H NMR spectrum (Fig. 1A). The block copolymer, mPEG-*b*-PDTG, was synthesized by ROP of DTG-NCA monomer using mPEG-NH₂ as the macroinitiator. The resultant mPEG-*b*-PDTG block copolymer was characterized by ¹H NMR spectrum and gel permeation chromatography (GPC). As shown in Fig. 1B, all proton resonance peaks of mPEG-*b*-PDTG were well assigned, and the degree of polymerization was calculated to be 52, according to the comparison of integral of proton g, h and proton f. In addition, GPC profile showed that the mPEG-*b*-PDTG had a unimodal peak with $M_n = 16,100$ g/mol and $D = 1.71$ (Fig. S5 in Supporting information). All these data demonstrated the successful ROP of DTG-NCA and the formation of mPEG-*b*-PDTG block copolymer.

The obtained amphiphilic mPEG-*b*-PDTG block copolymer can self-assemble into micelles in aqueous solution, consisting of a hydrophobic PDTG core and a hydrophilic PEG outer shell. The critical micelle concentration (CMC) of mPEG-*b*-PDTG micelles was determined to be 3.3×10^{-3} mg/mL by using pyrene as the fluorescence probe (Fig. S6 in Supporting information). Fig. 2A shows the results of dynamic light scattering (DLS) measurement of the micelles. The average diameter of the mPEG-*b*-PDTG micelle was 95 ± 3.2 nm. Moreover, the transmission electron microscopy (TEM) image indicated that the mPEG-*b*-PDTG micelles had a

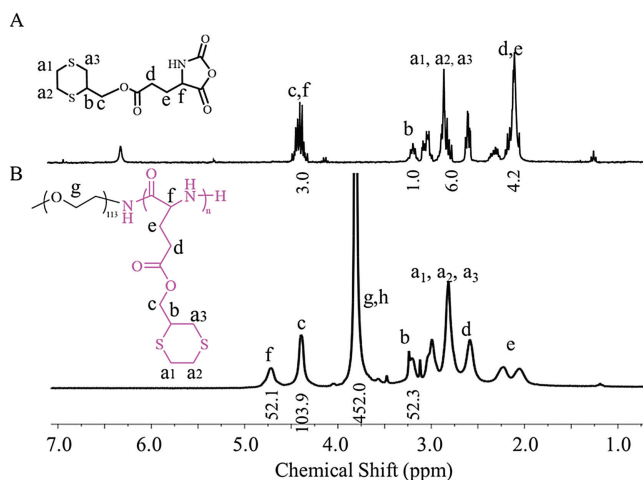


Fig. 1. Typical ¹H NMR spectra of DTG-NCA in CDCl₃ (A), and mPEG-*b*-PDTG in deuterated trifluoroacetic acid (B).

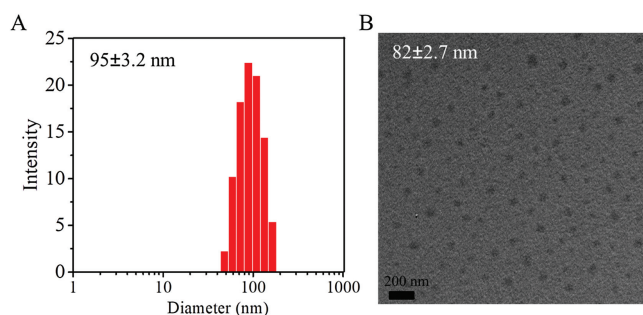
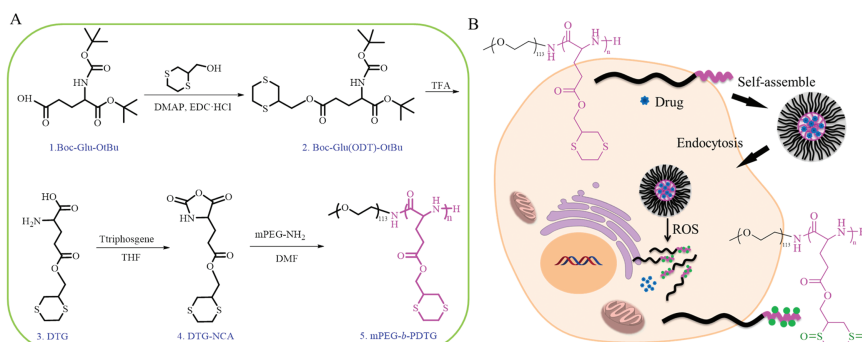


Fig. 2. DLS measurement (A) and TEM image (B) of the mPEG-*b*-PDTG micelles.

spherical morphology with a diameter of 82 ± 2.7 nm (Fig. 2B), which was slightly smaller than the diameter value determined by DLS. This should be due to that the micelles were in dehydrated state in TEM image, while the micelles were in hydrated state in DLS measurement.

It is well-documented that thioether-containing polymers are typical ROS-responsive materials; and usually, the hydrophobic thioether-containing polymer can be transformed into hydrophilic one *via* the oxidation conversion of hydrophobic thioether groups into hydrophilic sulfoxide and sulfone groups [27,28]. Thus, the mPEG-*b*-PDTG micelles are expected to have ROS-responsiveness. To test it, mPEG-*b*-PDTG micelles in aqueous solution were treated with or without H₂O₂, and then the particle sizes were monitored by DLS measurements at different time intervals. As shown in



Scheme 1. (A) Synthesis of mPEG-*b*-PDTG copolymer. (B) Schematic illustration of the self-assembly and intracellular drug release of mPEG-*b*-PDTG micelles.

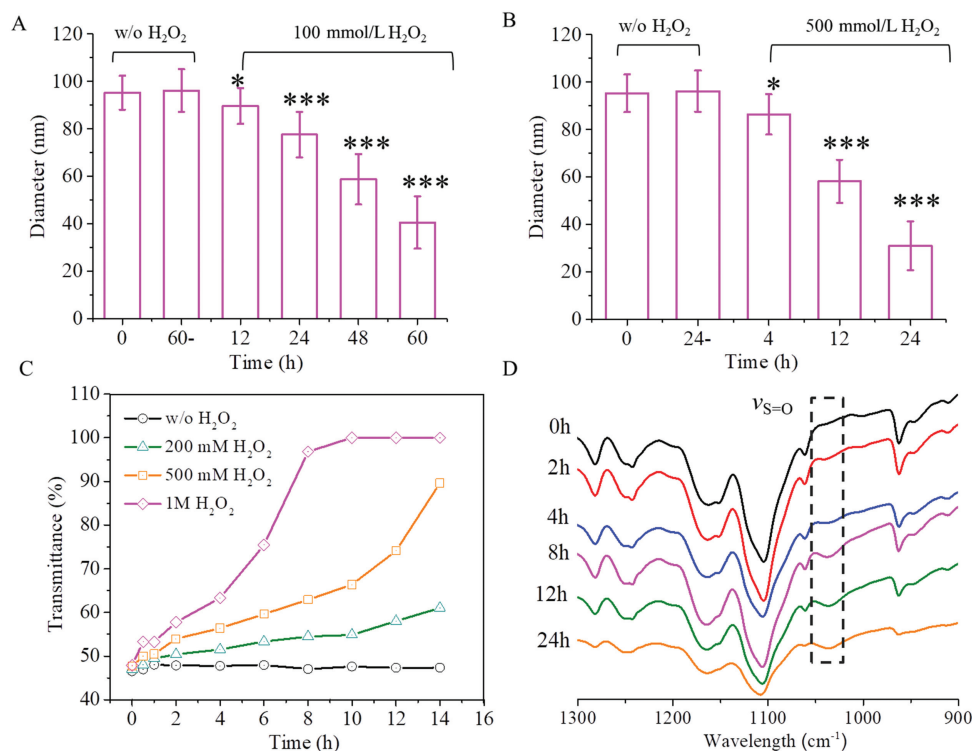


Fig. 3. Size changes of mPEG-*b*-PDTG micelles in the presence of (A) 100 mmol/L H₂O₂ and (B) 500 mmol/L H₂O₂ at 25 °C. * and *** indicate $P < 0.05$ and $P < 0.001$, respectively, compared with the w/o H₂O₂ group. (C) Plots of transmittance changes of mPEG-*b*-PDTG micelles solution (2.0 mg/mL) in the presence of different concentrations of H₂O₂. (D) 900–1300 cm⁻¹ FT IR window of the mPEG-*b*-PDTG micelles (1.0 mg/mL) after treatment with H₂O₂ (500 mmol/L) for different times. The intensity of all spectra was normalized against the ν_{as} CH₂ band at 2926 cm⁻¹.

Fig. 3A, when treated with 100 mmol/L H₂O₂, the size of mPEG-*b*-PDTG micelles decreased gradually to ~40 nm at 60 h and no valid DLS results could be obtained after 60 h. Moreover, a quicker decrease of sizes was observed when a higher concentration of H₂O₂ (500 mmol/L) was used (Fig. 3B). In contrast, negligible size variation was observed without treatment with H₂O₂ during the same period of time (Figs. 3A and B). All these results indicated that the mPEG-*b*-PDTG micelles were ROS-responsive and the disintegration of mPEG-*b*-PDTG micelles occurred upon treatment with H₂O₂. Furthermore, the TEM was applied to confirm the oxidation-induced disintegration of mPEG-*b*-PDTG micelles. As shown in Fig. S7 (Supporting information), irregular nano-aggregates were observed after incubation with H₂O₂ for 48 h, indicating the disintegration of micelles upon oxidation by H₂O₂.

Next, turbidity measurement was also performed to determine the ROS-responsive property of mPEG-*b*-PDTG micelles and, the results are shown in Fig. 3C. No transmittance changes could be observed in the absence of H₂O₂, while significant increases of transmittance were observed when treated with H₂O₂ (Fig. 3C and Fig. S8 in Supporting information). And the increases of transmittance would become quicker and more obvious for the micelles when a higher concentration of H₂O₂ was used. These results are consistent with the above-mentioned DLS measurements, which again suggest that the mPEG-*b*-PDTG micelles have excellent ROS-responsiveness.

To deeply understand the oxidation-responsiveness of mPEG-*b*-PDTG, the oxidation process of mPEG-*b*-PDTG was firstly characterized by FT-IR at different time intervals. As shown in Fig. 3D, a new peak at 1030 cm⁻¹, corresponding to S=O stretching vibration band, was clearly observed after incubation with H₂O₂ for 2 h, and becoming increasingly visible at prolonged incubation times. At the same time, no peaks ascribed to sulfones could be detected in FT-IR spectra. These results indicate that the thioethers

in mPEG-*b*-PDTG were oxidatively converted into sulfoxides by H₂O₂ (Fig. S9 in Supporting information), which is consistent with the previous report [24,28]. Next, the oxidation-induced structural change of 1,4-dithiane in the side chain was also investigated by ¹H NMR characterization by using DTM as the model molecule. It is clearly observed that the proton resonance signals at 2.63–2.99 ppm (a₁, a₂ and a₃) and 3.61 ppm (c) gradually change into corresponding proton resonance signals at 2.61–3.41 ppm (a'₁, a'₂ and a'₃) and 3.94 ppm (c') (Fig. S10 in Supporting information). The significant changes of chemical shift and peak shape also indicate the oxidation of thioethers into sulfoxides, which is in line with the FT-IR characterizations. Furthermore, the increased M_n of oxidized mPEG-*b*-PDTG was observed in GPC analysis, which further confirmed the oxidation-induced structural changes in the side chains (Fig. S5). Taken together, these results demonstrate that, upon treatment with H₂O₂, the thioether groups in the side chains can be oxidized into sulfoxide groups, which would result in the conversion of hydrophobic PDTG segment into hydrophilic polymer and subsequently lead to the disassembly of micelles.

To test the potential use of mPEG-*b*-PDTG for ROS-responsive drug release, Nile Red (NR), used as a model hydrophobic drug, was loaded into the micelles by a typical dialysis method, and the drug release behavior was monitored in the presence of different concentrations of H₂O₂. As shown in Fig. 4, there was almost no NR released from mPEG-*b*-PDTG micelles in the absence of H₂O₂, indicating the good stability of drug-loaded mPEG-*b*-PDTG micelles. In comparison, significant decreases of fluorescence, corresponding to the release of NR, were clearly observed in the presence of H₂O₂, and the higher concentration of H₂O₂ would result in quicker release of NR. This result should be ascribed to the H₂O₂-induced disintegration of the micelles that has been previously demonstrated by the DLS and turbidity measurements. In addition, the cellular uptake behavior of NR-loaded mPEG-*b*-

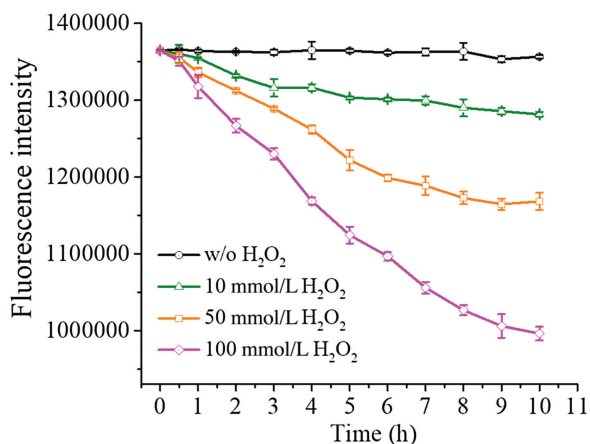


Fig. 4. The fluorescence intensity of NR-loaded mPEG-*b*-PDTG micelles monitored at different concentrations of H₂O₂.

PDTG micelles was further studied by confocal laser scanning microscopy. As shown in Fig. S11 (Supporting information), the NR fluorescence in cells gradually increased over time, indicating the efficient internalization of mPEG-*b*-PDTG micelles by MCF-7 cells. It has been reported that ROS, such as H₂O₂, superoxide and hydroxyl radical, are found to be overproduced in many types of pathological tissues, such as cancer and inflammation [10,11]. Therefore, these preliminary results suggest the promising use of mPEG-*b*-PDTG as a ROS-responsive drug delivery platform for treatment of cancer and other diseases [29–31].

Finally, the cell cytotoxicity of the obtained mPEG-*b*-PDTG copolymer in mouse melanoma B16F10 cells and mouse fibroblast L929 cells were tested by MTT assay. As shown in Figs. S12 and S13 (Supporting information), the mPEG-*b*-PDTG copolymer exhibited negligible cell cytotoxicity toward B16F10 cells or L929 cells (> 90% cell viability), even at a concentration as high as 500 μg/mL. Moreover, the oxidation product of mPEG-*b*-PDTG copolymer also showed no cytotoxic effects on L929 cells (Fig. S14 in Supporting information). These results suggest a good biocompatibility for the mPEG-*b*-PDTG copolymer.

In summary, we have successfully developed a new class of polypeptide bearing 1,4-dithiane pendants for ROS-responsive drug release. An amphiphilic block copolymer, mPEG-*b*-PDTG, was prepared *via* ROP of DTG-NCA and was capable to form micellar assemblies in aqueous solution. The mPEG-*b*-PDTG micelles underwent an oxidation-triggered disassembly due to the oxidation conversion of hydrophobic thioether group into hydrophilic sulfoxide group in the side chains. Then, the ROS-responsive drug

release capability of the mPEG-*b*-PDTG micelles was further demonstrated by using Nile Red as the model drug. In sum, with the facile synthetic process and good biocompatibility, the mPEG-*b*-PDTG copolymer may be promisingly used as a ROS-responsive drug delivery platform for treatment of cancer and other diseases.

Acknowledgments

This work was financially supported by National Key Research and Development Program of China (No. 2016YFC1100701), the National Natural Science Foundation of China (Nos. 51573184, 51520105004 and 51833010) and the Youth Innovation Promotion Association of Chinese Academy of Sciences (No. 2017266).

Appendix A. Supplementary data

Supplementary material related to this article can be found, in the online version, at doi:<https://doi.org/10.1016/j.cclet.2019.07.010>.

References

- [1] C.L. He, X.L. Zhuang, Z.H. Tang, H.Y. Tian, X.S. Chen, *Adv. Health. Mater.* 1 (2012) 48–78.
- [2] C. Deng, J. Wu, R. Cheng, et al., *Prog. Polym. Sci.* 39 (2014) 330–364.
- [3] H. Lu, J. Wang, Z. Song, et al., *Chem. Commun.* 50 (2014) 139–155.
- [4] W. Shen, P. He, C. Xiao, X. Chen, *Adv. Health. Mater.* 7 (2018) 1800354.
- [5] J. Zha, X. Jiang, *Chin. Chem. Lett.* 29 (2018) 1079–1087.
- [6] C. Xiao, J. Ding, C. He, X. Chen, *Acta Polym. Sin.* (2018) 45–55.
- [7] J. Huang, A. Heise, *Chem. Soc. Rev.* 42 (2013) 7373–7390.
- [8] T.J. Deming, *Chem. Rev.* 116 (2016) 786–808.
- [9] Y. Gao, C. Dong, *Chin. Chem. Lett.* 29 (2018) 927–930.
- [10] C.C. Winterbourn, *Nat. Chem. Biol.* 4 (2008) 278–286.
- [11] P.D. Ray, B.W. Huang, Y. Tsujii, *Cell. Signal.* 24 (2012) 981–990.
- [12] D. Trachootham, J. Alexandre, P. Huang, *Nat. Rev. Drug Discov.* 8 (2009) 579–591.
- [13] M. Schieber, Navdeep S. Chandel, *Curr. Biol.* 24 (2014) R453–R462.
- [14] C.C. Song, F.S. Du, Z.C. Li, *J. Mater. Chem. B* 2 (2014) 3413–3426.
- [15] C. Tapeinos, A. Pandit, *Adv. Mater.* 28 (2016) 5553–5585.
- [16] Q. Xu, C. He, C. Xiao, X. Chen, *Macromol. Biosci.* 16 (2016) 635–646.
- [17] J. Wang, Y. Zhang, E. Archibong, F.S. Ligler, Z. Gu, *Adv. Biosyst.* 1 (2017) 1700084.
- [18] W. Tao, Z. He, *Asian J. Pharm. Sci.* 13 (2018) 101–112.
- [19] J.R. Kramer, T.J. Deming, *J. Am. Chem. Soc.* 134 (2012) 4112–4115.
- [20] X. Fu, Y. Shen, W. Fu, Z. Li, *Macromolecules.* 46 (2013) 3753–3760.
- [21] J.R. Kramer, T.J. Deming, *J. Am. Chem. Soc.* 136 (2014) 5547–5550.
- [22] X. Fu, Y. Ma, J. Sun, Z. Li, *RSC Adv.* 6 (2016) 70243–70250.
- [23] X.H. Fu, Y.N. Ma, J. Sun, Z.B. Li, *Chinese J. Polym. Sci.* 34 (2016) 1436–1447.
- [24] Q. Xu, C. He, K. Ren, C. Xiao, X. Chen, *Adv. Health. Mater.* 5 (2016) 1979–1990.
- [25] S. Yu, C. Wang, J. Yu, et al., *Adv. Mater.* 30 (2018) 1801527.
- [26] C. Xiao, C. Zhao, P. He, et al., *Macromol. Rapid Comm.* 31 (2010) 991–997.
- [27] C. Xiao, J. Ding, L. Ma, et al., *Polym. Chem.* 6 (2015) 738–747.
- [28] P. Carampin, E. Lallana, J. Laliturai, et al., *Macromol. Chem. Phys.* 213 (2012) 2052–2061.
- [29] C. Wang, H. Sang, Y. Wang, et al., *Nano Lett.* 18 (2018) 7045–7051.
- [30] X. Li, Y. Zhang, Z. Ma, et al., *Chin. Chem. Lett.* 30 (2019) 489–493.
- [31] S. Gao, G. Tang, D. Hua, et al., *J. Mater. Chem. B* 7 (2019) 709–729.